REFINED CRITERIA TOWARD BOUNDEDNESS IN AN ATTRACTION-REPULSION CHEMOTAXIS SYSTEM WITH NONLINEAR PRODUCTIONS

Alessandro Columbu, Silvia Frassu and Giuseppe Viglialoro*

Dipartimento di Matematica e Informatica
Università di Cagliari
Via Ospedale 72, 09124. Cagliari (Italy)

Abstract. We study some zero-flux attraction-repulsion chemotaxis models, with nonlinear production rates for the chemore-pellent and the chemoattractant, whose formulation can be schematized as:

$$(\diamond) \quad \begin{cases} u_t = \Delta u - \chi \nabla \cdot (u \nabla v) + \xi \nabla \cdot (u \nabla w) & \text{in } \Omega \times (0, T_{max}), \\ \tau v_t = \Delta v - \varphi(t,v) + f(u) & \text{in } \Omega \times (0, T_{max}), \\ \tau w = \Delta w - \psi(t,w) + g(u) & \text{in } \Omega \times (0, T_{max}). \end{cases}$$

In this problem, Ω is a bounded and smooth domain of $\mathbb{R}^n$, for $n \geq 2$, $\chi, \xi > 0$, $f(u)$, $g(u)$ reasonably regular functions generalizing, respectively, the prototypes $f(u) = \alpha u^k$ and $g(u) = \gamma u^l$, for some $k, l, \alpha, \gamma > 0$ and all $u \geq 0$. Moreover, $\varphi(t,v)$ and $\psi(t,w)$ have specific expressions, $\tau \in \{0,1\}$ and $\Theta := \chi\alpha - \xi\gamma$. Once for any sufficiently smooth $u(x,0) = u_0(x) \geq 0$, $\tau v(x,0) = \tau v_0(x) \geq 0$ and $\tau w(x,0) = \tau w_0(x) \geq 0$ the local well posedness of problem $(\diamond)$ is ensured, we establish for the classical solution (u,v,w) defined in $\Omega \times (0, T_{max})$ that the life span is indeed $T_{max} = \infty$ and u, v and w are uniformly bounded in $\Omega \times (0,\infty)$ in the following cases:

I) For $\varphi(t,v) = \beta v$, $\beta > 0$, $\psi(t,w) = \delta w$, $\delta > 0$ and $\tau = 0$, provided
   I.1) $k < l$;
   I.2) $k, l \in \left(0, \frac{2}{n}\right)$;
   I.3) $k = l$ and $\Theta < 0$, or $l = k \in \left(0, \frac{2}{n}\right)$ and $\Theta \geq 0$.
II) For $\varphi(t,v) = \beta v$, $\beta > 0$, $\psi(t,w) = \delta w$, $\delta > 0$ and $\tau = 1$, whenever
   II.1) $l, k \in \left(0, \frac{1}{n}\right]$;
   II.2) $l \in \left(\frac{1}{n}, \frac{1}{n} + \frac{2}{n^2+4}\right)$ and $k \in \left(0, \frac{1}{n}\right]$, or $k \in \left(\frac{1}{n}, \frac{1}{n} + \frac{2}{n^2+4}\right)$ and $l \in \left(0, \frac{1}{n}\right]$;
   II.3) $l, k \in \left(\frac{1}{n}, \frac{1}{n} + \frac{2}{n^2+4}\right)$.
III) For $\varphi(t,v) = \frac{1}{|\Omega|}\int_\Omega f(u)$ and $\psi(t,w) = \frac{1}{|\Omega|}\int_\Omega g(u)$ and $\tau = 0$, under the assumptions $k < l$ or I.3).

In particular, in this paper we partially improve what derived in [31] and solve an open question given in [18]. Finally, the research is complemented with numerical simulations in bi-dimensional domains.

1. Introduction and motivations

1.1. **Presentation of the model.** This article is mainly dedicated to the following Cauchy boundary problem

$$(1) \quad \begin{cases} u_t = \Delta u - \chi \nabla \cdot (u \nabla v) + \xi \nabla \cdot (u \nabla w) & \text{in } \Omega \times (0, T_{max}), \\ \tau v_t = \Delta v - \beta v + f(u) & \text{in } \Omega \times (0, T_{max}), \\ \tau w_t = \Delta w - \delta w + g(u) & \text{in } \Omega \times (0, T_{max}), \\ u_\nu = v_\nu = w_\nu = 0 & \text{on } \partial\Omega \times (0, T_{max}), \\ u(x,0) = u_0(x), \ \tau v(x,0) = \tau v_0(x), \ \tau v(x,0) = \tau v_0(x) & x \in \bar{\Omega}, \end{cases}$$

defined in a bounded and smooth domain Ω of $\mathbb{R}^n$, with $n \geq 2$, $\chi, \xi, \beta, \delta > 0$, $\tau \in \{0,1\}$ and some functions $f = f(s)$ and $g = g(s)$, sufficiently regular in their argument $s \geq 0$, and essentially behaving as s^k and s^l, for some $k, l > 0$, and further regular initial data $u_0(x), \tau v_0(x), \tau w_0(x) \geq 0$. Moreover, u_ν (and similarly for v and w) indicates the outward normal derivative of u on $\partial\Omega$, whereas T_{max} identifies the maximum time up to which solutions to the system can be extended.

In conformity with the celebrated Keller–Segel models ([11, 12, 13]), if $u = u(x,t)$ stands for a certain population density (bacteria, organisms, cells) at the position x and at the time t, and $v = v(x,t)$ and $w = w(x,t)$ denote, respectively, the concentration of an attractive and repulsive chemical signal (chemoattractant and chemorepellent), model (1) idealizes the natural mechanism in which the automatic diffusion of the cells (the Laplacian Δu), initially distributed according to u_0, is perturbed by the aggregation/repulsion impact from the cross terms $\chi u \nabla v / \xi u \nabla w$ (increasing for larger values of χ and ξ). In addition, the initial distribution τv_0 (respectively, τw_0) of the chemoattractant (respectively, chemorepellent) diffuses and cells contribute to its growth in agreement to the law $f(u)$ (respectively, $g(u)$); the specified dynamics occurs in a totally impenetrable domain (homogeneous Neumann boundary conditions).

1.2. **A view on the state of the art.** In the context of the mentioned Keller–Segel model with single proliferative signal, problem (1) is a combination of this aggregative signal-production mechanism

$$(2) \qquad u_t = \Delta u - \chi \nabla \cdot (u \nabla v) \quad \text{and} \quad \tau v_t = \Delta v - v + u, \quad \text{in } \Omega \times (0, T_{max}),$$

and this repulsive signal-production one

$$(3) \qquad u_t = \Delta u + \xi \nabla \cdot (u \nabla w) \quad \text{and} \quad \tau w_t = \Delta v - u + w, \quad \text{in } \Omega \times (0, T_{max}).$$

Let us discuss some details on these problems and, since we will deal with classical solutions, we confine our attention to selected references; in this sense, we precise that the literature is richer.

From the one hand, if problem (2) is considered, since the attractive signal v increases with u, the inertial homogenization process of the cells' density could interrupt and very high and spatially concentrated spikes formations (*chemotactic collapse* or *blow-up at finite time*) may appear; this is especially due to the size of χ, the initial mass of the particle distribution, i.e., $m = \int_\Omega u_0(x)dx$, and the space dimension. Indeed, if in the one-dimensional setting blow-up phenomena are excluded (see [25]), in higher dimensions if $m\chi$ surpasses a certain critical value m_χ, the system might present the aforementioned chemotactic collapse, whereas for $m\chi < m_\chi$ no instability appears in the motion of the cells. There are many contributions dedicated to understanding this scenario. In this regard, in [6, 9, 23, 32] (and references therein cited), the interested reader can find pointers to the rich literature dealing with the existence and properties of global, uniformly bounded or blow-up (local) solutions to the Cauchy problem associated to (2). On the other hand, as far as nonlinear segregation chemotaxis models like those we are considering, when in problem (2) the segregation $f(u) = u$ is replaced by $f(u) \cong u^k$, with $0 < k < \frac{2}{n}$ ($n \geq 1$), uniform boundedness of all its solutions is proved in [17]. Moreover, by resorting to a simplified parabolic-elliptic version in spatially radial contexts, when the second equation is reduced to $0 = \Delta v - \frac{1}{|\Omega|} \int_\Omega f(u) + f(u)$, with $f(u) \cong u^k$, it is known (see [34]) that the same conclusion on the boundedness continues to be valid for any $n \geq 1$ and $0 < k < \frac{2}{n}$, whereas for $k > \frac{2}{n}$ blow-up phenomena may occur.

Indeed, from the other hand, the literature on model (3) is rather sparse and general (see, for instance, [21, 22] for analyses on similar contexts). In particular, no result on the blow-up scenario is available, and this is conceivable due to the repulsive nature of the mechanism.

Oppositely, quite different is the level of knowledge for attraction-repulsion chemotaxis problems accounting both (2) and (3); more exactly, in order to bring together precise results that can be compared each other, or at least discussed in a common spirit, we point out that *herein we prefer to focus on models exactly formulated as in* (1), otherwise the discussion might become too dispersive (see further comments in Remark 1). In the specific, we will consider not only analyses connected to the parabolic-elliptic-elliptic and the fully parabolic case of model (1), but also to a nonlocal version of the model itself.

The case $\tau = 0$. For linear growths of the chemoattractant and the chemorepellent, $f(u) = \alpha u$, $\alpha > 0$, and $g(u) = \gamma u$, $\gamma > 0$, we have that $\Theta := \chi\alpha - \xi\gamma$, value of the difference between the attraction and repulsion impacts, is such that whenever $\Theta < 0$ (repulsion-dominated regime), in any dimension all solutions to the model are globally bounded, whereas for $\Theta > 0$ (attraction-dominated regime) and $n = 2$ unbounded solutions can be detected (see [4, 16, 28, 30, 35] for some details on the issue). Indeed, for more general expressions of the proliferation laws, respectively f and g generalizing the prototypes $f(u) = \alpha u^k$, $k > 0$, and $g(u) = \gamma u^l$, $l > 0$, as far as we know the following are the most recent results, valid for $n \geq 2$ and derived in [31]: For every $\alpha, \beta, \gamma, \delta, \chi > 0$, and $l > k \geq 1$ (resp. $k > l \geq 1$), there exists $\xi^* > 0$ (resp. $\xi_* > 0$) such that if $\xi > \xi^*$ (resp. $\xi \geq \xi_*$), any sufficiently regular initial datum $u_0(x) \geq 0$ (resp. $u_0(x) \geq 0$ small in some Lebesgue space) emanates a unique classical solution, uniformly bounded in time. Moreover, the same conclusion continues valid for any $\alpha, \beta, \gamma, \delta, \chi, \xi > 0$, any sufficiently regular $u_0(x) \geq 0$ if the hypotheses $0 < k < 1$ and $l = 1$ are accomplished.

The case $\tau = 1$. First, we point out that in the context of real applications model (1) was introduced in [19] for one-dimensional settings and linear proliferation, to describe the aggregation of microglia observed in Alzheimer's disease.

Moreover, from the stricter mathematical point of view, in [28] it is proved that in two-dimensional domains, for $f(u) = \alpha u$ and $g(u) = \gamma u$, sufficiently smooth initial data generate global-in-time bounded solutions whenever (recall $\Theta = \chi\alpha - \xi\gamma$)

$$\Theta < 0 \quad \text{and} \quad \beta = \delta \quad \text{or} \quad \Theta < 0 \quad \text{and} \quad -\frac{\chi^2\alpha^2(\beta - \delta)^2}{2\Theta\beta^2 C} \int_\Omega u_0(x) \leq 1, \quad \text{for some } C > 0.$$

Finally, there are very few blow-up results in the same frame of the researches herein mentioned; we are aware of [15], where unbounded solutions in three-dimensional radially symmetrical domains are constructed in the attraction-dominated regime, that is $\Theta > 0$.

The nonlocal case. If we take into account this nonlocal version of model (1)

$$
(4) \quad
\begin{cases}
u_t = \Delta u - \chi \nabla \cdot (u \nabla v) + \xi \nabla \cdot (u \nabla w) & \text{in } \Omega \times (0, T_{max}), \\
0 = \Delta v - \frac{1}{|\Omega|} \int_\Omega f(u) + f(u) & \text{in } \Omega \times (0, T_{max}), \\
0 = \Delta w - \frac{1}{|\Omega|} \int_\Omega g(u) + g(u) & \text{in } \Omega \times (0, T_{max}), \\
u_\nu = v_\nu = w_\nu = 0 & \text{on } \partial\Omega \times (0, T_{max}), \\
u(x,0) = u_0(x) & x \in \bar\Omega, \\
\int_\Omega v(x,t) dx = \int_\Omega w(x,t) dx = 0 & t \in (0, T_{max}),
\end{cases}
$$

in [18] it is established that if $k > l$ and $k > \frac{2}{n}$, there are initial data producing solutions blowing up at some finite time while, for any $l > 0$, if $0 < k < \frac{2}{n}$ such a phenomenon is prevented and all solutions are globally bounded in time. For the sake of clarity, in this model v represents the *deviation* of the chemical signal (and not the chemical substance itself, as previously indicated). In particular, since the deviation measures the difference between the signal concentration and its mean, to be rigorous we would substitute in the model v with $\bar v$, being $\bar v = v - \frac{1}{|\Omega|} \int_\Omega v$. We avoid this relabeling, but we observe that conversely to what happens to the cell and chemical densities (which are nonnegative) the *deviation* changes sign. In particular, from its definition, it is suddenly seen that its mean is zero (as fixed in the last assumptions of model (4)), which in turn ensures the uniqueness of the solution for the Poisson equation under homogeneous Neumann boundary conditions. Exactly the same explanation is valid for w.

Remark 1 (Studies in close contexts to model (1)). *The reason why we are putting our attention to models where diffusion and both sensitivities are linear and no logistic source perturbs the overall dynamics of the cells's density, as in the first equation of (1), is due to the consideration that when this is replaced with*

$$
(5) \quad u_t = \nabla(\cdot D(u)\nabla u - S(u)\nabla v + T(u)\nabla w) + h(u),
$$

for some $D(u), S(u), T(u)$ and $h(u)$, the overall mathematical analysis is in some sense more manageable. Indeed, for standard situations where $D(u) \simeq u^{m_1}, S(u) \simeq u^{m_2}, T(u) \simeq u^{m_3}$ and $h(u) \simeq \lambda u - \mu u^\vartheta$ (where $m_1, m_2, m_3, \lambda, \mu, \vartheta$ assume some real values), the technical machinery involving functional and algebraic inequalities is more inclined to work exactly due to the leeway given by those parameters. Naturally, this room for maneuver is much more reduced when the parameters are fixed and the specific model is not always recoverable from the more general one; moreover no direct comparison between the two formulations is strictly possible.

Despite that, we herein give hints to the most recent outcomes obtained in models close to (1). For linear diffusion and sensitivities, linear and nonlinear productions and logistic terms, criteria toward boundedness, long time behaviors and blow-up issues for related solutions to (1) in the case $\tau = 0$, are studied in [7, 36, 2]. Similar analyses, in the case $\tau = 1$, are discussed in [27]. Finally, moving to scenarios where the particles' density obeys an equation as (5), with D, S, T, h behaving as specified, for both the cases $\tau = 0$ and $\tau = 1$ for the equation of v and w perturbed by general proliferation laws, we suggest the interesting paper [26].

2. CLAIMS OF THE THEOREMS

In this research we aim at extending the mathematical comprehension of attraction-repulsion Keller–Segel systems with linear diffusion and sensitivity and without logistics, by giving answers to questions not yet covered in the literature or improving already established results.

To this scope, once these hypotheses are fixed

$$
(6) \quad f, g \in C^1([0,\infty)) \quad \text{with} \quad 0 \le f(s) \le \alpha s^k \text{ and } \gamma_0(1+s)^l \le g(s) \le \gamma_1(1+s)^l, \quad \text{for some } \alpha, k, l > 0, \gamma_1 \ge \gamma_0 > 0,
$$

what follows is proved.

Theorem 2.1. *Let Ω be a smooth and bounded domain of $\mathbb{R}^n$, with $n \ge 2$, $\tau = 0$ and χ, ξ, β, δ positive. Moreover, for some $\alpha, \gamma_0, \gamma_1 > 0$, let f and g comply with assumptions (6) in at least one of these situations:*
   (1) $k < l$;
   (2) $k, l \in \left(0, \frac{2}{n}\right)$;
   (3) $k = l$ and $\Theta_0 := \chi\alpha - \xi\gamma_0 < 0$, or $l = k \in \left(0, \frac{2}{n}\right)$ and $\Theta_0 \ge 0$.
Then for any initial data $u_0 \in W^{1,\infty}(\bar\Omega)$, with $u_0 \ge 0$ on $\bar\Omega$, problem (1) admits a unique global and uniformly bounded classical solution.

Theorem 2.2. *Let Ω be a smooth and bounded domain of $\mathbb{R}^n$, with $n \ge 2$, $\tau = 1$ and χ, ξ, β, δ positive. Moreover, for some $\alpha, \gamma_0, \gamma_1 > 0$, let f and g comply with assumptions (6) in at least one of these situations:*
   (1) $l, k \in \left(0, \frac{1}{n}\right]$;
   (2) $l \in \left(\frac{1}{n}, \frac{1}{n} + \frac{2}{n^2+4}\right)$ and $k \in \left(0, \frac{1}{n}\right]$, or $k \in \left(\frac{1}{n}, \frac{1}{n} + \frac{2}{n^2+4}\right)$ and $l \in \left(0, \frac{1}{n}\right]$;
   (3) $l, k \in \left(\frac{1}{n}, \frac{1}{n} + \frac{2}{n^2+4}\right)$.

Then for any initial data $(u_0, v_0, w_0) \in (W^{1,\infty}(\Omega))^3$, *with* $u_0, v_0, w_0 \geq 0$ *on* $\bar{\Omega}$, *problem* (1) *admits a unique global and uniformly bounded classical solution.*

Theorem 2.3. *Let* Ω *be a smooth and bounded domain of* $\mathbb{R}^n$, *with* $n \geq 2$, *and* χ, ξ *positive. Moreover, for some* $\alpha, \gamma_0, \gamma_1 > 0$, *let* f *and* g *comply with hypotheses* (6), *for* $k < l$, *or for* $k = l$ *and* $\Theta_0 := \chi\alpha - \xi\gamma_0 < 0$, *or for* $l = k \in \left(0, \frac{2}{n}\right)$ *and* $\Theta_0 \geq 0$. *Then for any initial data* $u_0 \in W^{1,\infty}(\bar{\Omega})$, *with* $u_0 \geq 0$ *on* $\bar{\Omega}$, *problem* (4) *admits a unique global and uniformly bounded classical solution.*

Remark 2 (Solving an open question and improvements of known results)**.** *Let us give these comments:*
  ▷ *After [18, Theorem 1.2], precisely in [18, Remark 1.2], the authors leave an open question by textually writing: "we still have no ideas for the behavior of the solution in the case* $k > \frac{2}{n}$ *and* $k < l$.". *The statement of Theorem* 2.3 *provides the answer to this question and these two theorems give a more complete picture on the behavior of solutions to model* (4).
  ▷ *The condition* $l > k > 0$ *derived in Theorem* 2.1, *and yielding boundedness to model* (1), *improves that in [31, Theorem 4.4].*

Remark 3. *As usual in the nomenclature, in chemotaxis models a global and uniformly bounded classical solution to problem* (1) *is a triplet of nonnegative functions*

(7) $$u, v, w \in C^0(\bar{\Omega} \times [0, \infty)) \cap C^{2,1}(\bar{\Omega} \times (0, \infty)) \cap L^\infty((0, \infty); L^\infty(\Omega)).$$

The rest of the paper is structured as follows. First, in §3 we give some indications concerning the local existence and uniqueness of a classical solution to model (1) and some of its main properties. In this same section we recall a *boundedness criterion*, establishing globality and boundedness of local solutions from proper *a priori* L^p-boundedness, which is achieved in §5 by relying on preliminaries collected in §4. In the same §5 we can deduce the claims of Theorems 2.1, 2.2 and 2.3. Finally, in §6, the theoretical results presented here are numerically investigated in planar domains.

3. EXISTENCE OF LOCAL-IN-TIME SOLUTIONS AND MAIN PROPERTIES

From now on we will tacitly assume that all the appearing constants below c_i, $i = 1, 2, \ldots$, *are positive.*

Once Ω, χ, ξ and f, g are fixed and obey what hypothesized above, (u, v, w) will stand for the classical and nonnegative solution to problem (1) (or (4)), defined for all $(x, t) \in \bar{\Omega} \times [0, T_{max})$, for some finite T_{max}, and emanating from nonnegative initial data $u_0, \tau v_0, \tau w_0 \in W^{1,\infty}(\Omega)$. In particular, u, v and w are such that

(8) $$\int_\Omega u(x,t)dx = \int_\Omega u_0(x)dx = m \quad \text{on } (0, T_{max}),$$

and

(9) $$f(u) \in L^\infty((0, T_{max}); L^{\frac{1}{k}}(\Omega)) \quad \text{and} \quad g(u) \in L^\infty((0, T_{max}); L^{\frac{1}{l}}(\Omega)), \text{ whenever } k, l \in (0, 1].$$

Further, globality and boundedness of (u, v, w) (in the sense of (7)) are ensured whenever (*boundedness criterion*, below) $u \in L^\infty((0, T_{max}); L^p(\Omega))$, with some $p > 1$ large, and uniformly with respect $t \in (0, T_{max})$: formally,

(10) $$\text{If } \exists L > 0, p > \frac{n}{2} \ \Big| \ \int_\Omega u^p \leq L \text{ on } (0, T_{max}) \Rightarrow (u, v, w) \in (L^\infty((0, \infty); L^\infty(\Omega)))^3.$$

Since the arguments concerning local existence and boundedness criterion are standard, we do not justify them nor dedicate any lemma; details are achievable in [28] and [29, Appendix A.].

Conversely, the mass conservation property (8) comes from an integration over Ω of the first equation in problem (1). On the other hand, from this bound we have (9) by noticing that

(11) $$\int_\Omega f(u)^{\frac{1}{k}} \leq \alpha^{\frac{1}{k}} \int_\Omega u = c_1 \quad \text{and similarly} \int_\Omega g(u)^{\frac{1}{l}} \leq c_2 \text{ for all } t \in (0, T_{max}).$$

Inclusions (9), as well as relations (11), will be of crucial importance when we analyze properties of solutions to the fully parabolic model (1). In particular, parabolic regularity theory allows to derive this result, which provides some uniform bounds for $\|v(\cdot, t)\|_{W^{1,r}(\Omega)}$ and $\|w(\cdot, t)\|_{W^{1,s}(\Omega)}$, with $r, s \geq 1$.

Lemma 3.1. *We have that* v *and* w *are such that*

$$\int_\Omega |\nabla v(\cdot, t)|^r \leq c_3 \quad \text{on } (0, T_{max}) \begin{cases} \text{for all } r \in [1, \infty) & \text{if } k \in \left(0, \frac{1}{n}\right], \\ \text{for all } r \in \left[1, \frac{n}{nk-1}\right) & \text{if } k \in \left(\frac{1}{n}, 1\right], \end{cases}$$

and

$$\int_\Omega |\nabla w(\cdot, t)|^s \leq c_4 \quad \text{on } (0, T_{max}) \begin{cases} \text{for all } s \in [1, \infty) & \text{if } l \in \left(0, \frac{1}{n}\right], \\ \text{for all } s \in \left[1, \frac{n}{nl-1}\right) & \text{if } l \in \left(\frac{1}{n}, 1\right]. \end{cases}$$

Proof. The proof takes into account inclusions (9) and, depending on τ, it is consequence of elliptic or parabolic regularity results; see, for instance, [1] and [14, 8]. □

4. Some preparatory tools

In this section we collect some inequalities and further necessary results.

Lemma 4.1. *Let $A, B \geq 0$, $d_1, d_2 > 0$ and $p > 1$. Then for some $d, d_3 > 0$ we have*

$$
(12) \qquad A^{d_1} + B^{d_2} \geq 2^{-d}(A + B)^d - d_3,
$$

and

$$
(13) \qquad (A + B)^p \leq 2^{p-1}(A^p + B^p).
$$

Moreover, let $d_4, d_5 > 0$ be such that $d_4 + d_5 < 1$. Then for all $\epsilon > 0$

$$
(14) \qquad A^{d_4} B^{d_5} \leq \epsilon(A + B) + c_5.
$$

Proof. The proofs are available, respectively, in [**20**, Lemma 3.3], [**10**, Theorem 1] and [**3**, Lemma 4.3]. $\square$

Lemma 4.2. *Let $\Omega \subset \mathbb{R}^n$, $n \geq 1$, be a bounded and smooth domain and $\delta > 0$. Then for any nonnegative $g \in C^1(\bar{\Omega})$, the solution $0 \leq \psi \in C^{2,\kappa}(\bar{\Omega})$, $0 < \kappa < 1$, of the problem*

$$
\begin{cases} 0 = \Delta\psi + g - \delta\psi & in \ \Omega, \\ \psi_\nu = 0 & on \ \partial\Omega, \end{cases}
$$

has the following property: For any $\hat{c}, \sigma > 0$ and $\bar{p} \in (1, \infty)$, there exists $\tilde{c} = \tilde{c}(\sigma, \bar{p}) > 0$ such that

$$
(15) \qquad \hat{c} \int_\Omega \psi^{\bar{p}+1} \leq \sigma \int_\Omega g^{\bar{p}+1} + \frac{\tilde{c}}{|\Omega|^{\bar{p}}} \left(\int_\Omega g \right)^{\bar{p}+1}.
$$

Proof. A detailed proof of (15) can be found in [**31**, Lemma 3.1]. (See also [**33**, Lemma 2.2].) $\square$

5. A priori estimates and proof of the theorems

Let (u, v, w) be the local classical solution to models (1) and (4). Whenever we show that $u \in L^\infty((0, T_{max}); L^p(\Omega))$, for some $p > \frac{n}{2}$, we can take advantage from the boundedness criterion given in (10) and directly obtain that, indeed, $u \in L^\infty((0, \infty); L^\infty(\Omega))$; as an immediate consequence of that, regularity theories applied to the equations of v and w entail that also v, w belong to $L^\infty((0, \infty); L^\infty(\Omega))$.

So our goal in this section is showing the inclusion $u \in L^\infty((0, T_{max}); L^p(\Omega))$, for some $p > \frac{n}{2}$; we will prove this by establishing an absorptive differential inequality for the functional $y(t) := \int_\Omega u^p$. To be precise, we aim at deriving this inequality for y

$$
(16) \qquad y'(t) + c_6 \int_\Omega |\nabla u^{\frac{p}{2}}|^2 \leq c_7 \quad \text{on } (0, T_{max}).
$$

In fact, at this point, we can successively exploit the Gagliardo–Nirenberg inequality (see [**24**]) combined with (13) (used in the sequel without mentioning), so to write

$$
\int_\Omega u^p = ||u^{\frac{p}{2}}||^2_{L^2(\Omega)} \leq c_8 ||\nabla u^{\frac{p}{2}}||^{2\theta}_{L^2(\Omega)} ||u^{\frac{p}{2}}||^{2(1-\theta)}_{L^{\frac{2}{p}}(\Omega)} + c_8 ||u^{\frac{p}{2}}||^2_{L^{\frac{2}{p}}(\Omega)} \qquad \text{for all } t \in (0, T_{max}),
$$

with

$$
0 < \theta = \frac{\frac{np}{2}(1 - \frac{1}{p})}{1 - \frac{n}{2} + \frac{np}{2}} < 1.
$$

In turn, by taking into consideration bound (8), the above inequality leads to

$$
(17) \qquad \int_\Omega u^p \leq c_9 \left(\int_\Omega |\nabla u^{\frac{p}{2}}|^2 \right)^\theta + c_9 \quad \text{on } (0, T_{max}),
$$

so that by manipulating it and inserting the result into (16), we can observe also by virtue of (12) that y satisfies this initial problem

$$
\begin{cases} y'(t) \leq c_{10} - c_{11} y^{\frac{1}{\theta}}(t) & \text{for all } t \in (0, T_{max}), \\ y(0) = \int_\Omega u_0^p. \end{cases}
$$

Consequently, an ODE comparison principle implies that $\int_\Omega u^p \leq \max \left\{ y(0), \left(\frac{c_{10}}{c_{11}} \right)^\theta \right\} := L$ for all $t \in (0, T_{max})$, providing the desired inclusion.

Analysis of solutions to model (1) with $\tau = 0$; proof of Theorem 2.1.

Lemma 5.1. *Let either $0 < k < l$ or $k, l \in \left(0, \frac{2}{n}\right)$. Then for any $p > \max\left\{l, \frac{l(nl-2)}{n}, \frac{n}{2}\right\}$, u fulfills for some $L > 0$*

$$(18) \qquad \int_\Omega u^p \leq L \quad \text{for all} \quad t \in (0, T_{max}).$$

Moreover, we have the same conclusion if $k = l$ and $\chi\alpha - \xi\gamma_0 < 0$, or $l = k \in \left(0, \frac{2}{n}\right)$ and $\chi\alpha - \xi\gamma_0 \geq 0$.

Proof. By testing the first equation of problem (1) with u^{p-1}, using its boundary conditions and taking into account the second and the third equation, we have

$$\frac{d}{dt}\int_\Omega u^p = p\int_\Omega u^{p-1}u_t = -p(p-1)\int_\Omega u^{p-2}|\nabla u|^2 - (p-1)\chi\int_\Omega u^p(v - f(u)) + (p-1)\xi\int_\Omega u^p(w - g(u))$$

$$\leq -p(p-1)\int_\Omega u^{p-2}|\nabla u|^2 + (p-1)\chi\int_\Omega u^p f(u) + (p-1)\xi\int_\Omega u^p w - (p-1)\xi\int_\Omega u^p g(u) \quad \text{on} \ (0, T_{max}).$$

Now, we recall the definitions of f and g given in (6), exploit $u < (u+1)$ and inequality (13) so to obtain

$$(19) \quad \begin{aligned} \frac{d}{dt}\int_\Omega u^p &\leq -p(p-1)\int_\Omega u^{p-2}|\nabla u|^2 + (p-1)\chi\alpha\int_\Omega u^{p+k} + (p-1)\xi\int_\Omega u^p w - (p-1)\xi\gamma_0\int_\Omega u^p(u+1)^l \\ &\leq -p(p-1)\int_\Omega u^{p-2}|\nabla u|^2 + (p-1)\chi\alpha\int_\Omega u^{p+k} + (p-1)\xi\int_\Omega u^p w - (p-1)\xi\gamma_0\int_\Omega u^{p+l} \quad \text{for all} \ t \in (0, T_{max}). \end{aligned}$$

As to the third integral on the right-hand side of (19), an application of Young's inequality, Lemma 4.2 with $\psi = w$ and $\bar{p} = \frac{p}{l} > 1$ and relation (13) provide for $\epsilon_1, \sigma, \tilde{\sigma} > 0$

$$(20) \quad \begin{aligned} (p-1)\xi\int_\Omega u^p w &\leq \epsilon_1\int_\Omega u^{p+l} + c_{12}\int_\Omega w^{\bar{p}+1} \leq \epsilon_1\int_\Omega u^{p+l} + \sigma\int_\Omega (g(u))^{\bar{p}+1} + c_{13}\left(\int_\Omega g(u)\right)^{\bar{p}+1} \\ &\leq \epsilon_1\int_\Omega u^{p+l} + \sigma\int_\Omega (\gamma_1(u+1)^l)^{\bar{p}+1} + c_{13}\left(\int_\Omega \gamma_1(u+1)^l\right)^{\bar{p}+1} \\ &\leq \epsilon_1\int_\Omega u^{p+l} + \tilde{\sigma}\int_\Omega u^{l(\bar{p}+1)} + c_{14}\left(\int_\Omega u^l\right)^{\bar{p}+1} + c_{15} \quad \text{on} \ (0, T_{max}). \end{aligned}$$

If $l \in (0, 1]$ the last integral in (20) is controlled by a constant thanks Hölder's inequality and the mass conservation property (8). On the other hand, if $l > 1$ we can estimate the term $\left(\int_\Omega u^l\right)^{\bar{p}+1}$ by applying the Gagliardo–Nirenberg inequality, in this way:

$$c_{14}\left(\int_\Omega u^l\right)^{\frac{p+l}{l}} = c_{14}\|u^{\frac{p}{2}}\|_{L^{\frac{2l}{p}}(\Omega)}^{\frac{2(p+l)}{p}} \leq c_{16}\|\nabla u^{\frac{p}{2}}\|_{L^2(\Omega)}^{\frac{2(p+l)}{p}\theta_1}\|u^{\frac{p}{2}}\|_{L^{\frac{2}{p}}(\Omega)}^{\frac{2(p+l)}{p}(1-\theta_1)} + c_{16}\|u^{\frac{p}{2}}\|_{L^{\frac{2}{p}}(\Omega)}^{\frac{2(p+l)}{p}} \quad \text{for all} \ t \in (0, T_{max}),$$

where for p as in our assumptions we have

$$0 < \theta_1 = \frac{1 - \frac{1}{l}}{1 + \frac{2}{np} - \frac{1}{p}} < 1 \quad \text{and} \quad 0 < \frac{(p+l)}{p}\theta_1 < 1.$$

Hence, by recalling the mass conservation property (8), the Young and above inequalities entail for any $\epsilon_2 > 0$

$$(21) \qquad c_{14}\left(\int_\Omega u^l\right)^{\frac{p+l}{l}} \leq c_{17}\left(\int_\Omega |\nabla u^{\frac{p}{2}}|^2\right)^{\frac{(p+l)}{p}\theta_1} + c_{17} \leq \epsilon_2\int_\Omega |\nabla u^{\frac{p}{2}}|^2 + c_{18} \quad \text{on} \ (0, T_{max}).$$

As a consequence, for any $l > 0$, by putting estimates (20) and (21) into (19) we get for all $t \in (0, T_{max})$

$$(22) \qquad \frac{d}{dt}\int_\Omega u^p \leq -p(p-1)\int_\Omega u^{p-2}|\nabla u|^2 + (p-1)\chi\alpha\int_\Omega u^{p+k} + (\epsilon_1 + \tilde{\sigma} - (p-1)\xi\gamma_0)\int_\Omega u^{p+l} + \epsilon_2\int_\Omega |\nabla u^{\frac{p}{2}}|^2 + c_{19}.$$

Now we analyze the case $0 < k < l$; by applying the Young inequality to the second integral at the right-hand side of the above estimate yields for $\epsilon_3 > 0$

$$(p-1)\chi\alpha\int_\Omega u^{p+k} \leq \epsilon_3\int_\Omega u^{p+l} + c_{20} \quad \text{for all} \ t \in (0, T_{max}),$$

so that, by plugging the latter into (22), and also in view of the identity

$$\int_\Omega u^{p-2}|\nabla u|^2 = \frac{4}{p^2}\int_\Omega |\nabla u^{\frac{p}{2}}|^2 \quad \text{on} \ (0, T_{max}),$$

we have

$$\frac{d}{dt}\int_\Omega u^p \leq \left(\epsilon_2 - \frac{4(p-1)}{p}\right)\int_\Omega |\nabla u^{\frac{p}{2}}|^2 + (\epsilon_1 + \tilde{\sigma} + \epsilon_3 - (p-1)\xi\gamma_0)\int_\Omega u^{p+l} + c_{21} \quad \text{on} \ (0, T_{max}).$$

Finally, by choosing $\epsilon_1, \epsilon_2, \epsilon_3, \tilde{\sigma}$ such that $\epsilon_2 < \frac{4(p-1)}{p}$ and $\epsilon_1 + \tilde{\sigma} + \epsilon_3 \le (p-1)\xi\gamma_0$, we arrive at similar inequality as in (16). (Note that in the case $l \in (0,1]$ one can directly take $\epsilon_2 = 0$.)

Let turn our attention to the case $l, k \in \left(0, \frac{2}{n}\right)$. Thanks to the Gagliardo–Nirenberg inequality and to the mass conservation property (8), the estimate of the second integral of the right-hand side of (22) becomes

$$(p-1)\chi\alpha \int_\Omega u^{p+k} = (p-1)\chi\alpha \|u^{\frac{p}{2}}\|_{L^{\frac{2(p+k)}{p}}(\Omega)}^{\frac{2(p+k)}{p}} \le c_{22}\|\nabla u^{\frac{p}{2}}\|_{L^2(\Omega)}^{\frac{2(p+k)}{p}\theta_2}\|u^{\frac{p}{2}}\|_{L^{\frac{2}{p}}(\Omega)}^{\frac{2(p+k)}{p}(1-\theta_2)} + c_{22}\|u^{\frac{p}{2}}\|_{L^{\frac{2}{p}}(\Omega)}^{\frac{2(p+k)}{p}}$$

$$\le c_{23}\left(\int_\Omega |\nabla u^{\frac{p}{2}}|^2\right)^{\frac{(p+k)}{p}\theta_2} + c_{23} \quad \text{on } (0, T_{max}),$$

where

$$\theta_2 = \frac{\frac{p}{2} - \frac{p}{2(p+k)}}{\frac{p}{2} + \frac{1}{n} - \frac{1}{2}} \in (0,1).$$

Since $\frac{(p+k)}{p}\theta_2 < 1$ for $0 < k < \frac{2}{n}$, an application of the Young inequality gives for $\epsilon_4 > 0$

$$(23) \qquad\qquad (p-1)\chi\alpha \int_\Omega u^{p+k} \le \epsilon_4 \int_\Omega |\nabla u^{\frac{p}{2}}|^2 + c_{24} \quad \text{for all } t \in (0, T_{max}).$$

By plugging this gained estimate into bound (22), we reason as above and the arbitrariness of the constants associated to the terms $\int_\Omega |\nabla u^{\frac{p}{2}}|^2$ and $\int_\Omega u^{p+l}$ allows us to establish for $y(t)$ an estimate as in (16).

Finally, if we take $k = l$ in (22), we arrive at the following estimate:

$$\frac{d}{dt}\int_\Omega u^p \le -p(p-1)\int_\Omega u^{p-2}|\nabla u|^2 + ((p-1)(\chi\alpha - \xi\gamma_0) + \epsilon_1 + \tilde{\sigma})\int_\Omega u^{p+l} + \epsilon_2 \int_\Omega |\nabla u^{\frac{p}{2}}|^2 + c_{19} \quad \text{for all } t \in (0, T_{max}).$$

If $\chi\alpha - \xi\gamma_0 < 0$, for proper constant $\epsilon_1, \tilde{\sigma}$, we can make $(p-1)(\chi\alpha - \xi\gamma_0) + \epsilon_1 + \tilde{\sigma} \le 0$ and consequently neglect the term associated to $\int_\Omega u^{p+l}$; on the other hand if $\chi\alpha - \xi\gamma_0 \ge 0$ and $l \in \left(0, \frac{2}{n}\right)$ we may treat such integral similarly to (23). In both cases we conclude. $\qquad \square$

Analysis of solutions to model (4); proof of Theorem 2.3.

Lemma 5.2. *Let $l > 1$ and $k < l$. Then there exists $q > l$ such that whenever $p > \max\{\frac{q}{n}(qn-2), \frac{n}{2}\}$ we have that u obeys the same relation in (18), possibly with a different constant L.*

Moreover, the same conclusion holds true whenever either $l \in (0,1]$ and $k < l$, or $k = l$ and $\chi\alpha - \xi\gamma_0 < 0$, or $l = k \in \left(0, \frac{2}{n}\right)$ and $\chi\alpha - \xi\gamma_0 \ge 0$.

Proof. By reasoning as in the proof of Lemma 5.1, we deduce the following estimate on $(0, T_{max})$:

$$\frac{d}{dt}\int_\Omega u^p = -p(p-1)\int_\Omega u^{p-2}|\nabla u|^2 - (p-1)\chi\int_\Omega u^p\left(\frac{1}{|\Omega|}\int_\Omega f(u) - f(u)\right) + (p-1)\xi\int_\Omega u^p\left(\frac{1}{|\Omega|}\int_\Omega g(u) - g(u)\right)$$

$$(24) \qquad \le -p(p-1)\int_\Omega u^{p-2}|\nabla u|^2 + (p-1)\chi\alpha\int_\Omega u^{p+k} + \frac{(p-1)\xi}{|\Omega|}\int_\Omega g(u)\int_\Omega u^p - (p-1)\xi\gamma_0\int_\Omega u^{p+l}$$

$$\le -p(p-1)\int_\Omega u^{p-2}|\nabla u|^2 + (p-1)\chi\alpha\int_\Omega u^{p+k} + c_{25}\int_\Omega u^p + c_{26}\int_\Omega u^l\int_\Omega u^p - (p-1)\xi\gamma_0\int_\Omega u^{p+l}.$$

Since $k < l$, by exploiting Young's inequality we obtain for $\epsilon_5 > 0$

$$(p-1)\chi\alpha \int_\Omega u^{p+k} \le \epsilon_5 \int_\Omega u^{p+l} + c_{27} \quad \text{on } (0, T_{max}).$$

If $0 < l \le 1$, the product of the two integrals $\int_\Omega u^l \int_\Omega u^p$ in (24) can be treated by exploiting the mass conservation property (8) and bound (17), so to get for $\epsilon_6 > 0$

$$\int_\Omega u^l \int_\Omega u^p \le c_{28}\int_\Omega u^p \le \epsilon_6 \int_\Omega |\nabla u^{\frac{p}{2}}|^2 + c_{29} \quad \text{for all } t \in (0, T_{max}).$$

On the other hand, if $l > 1$ a twice application of the Hölder inequality gives

$$\int_\Omega u^l \int_\Omega u^p \le c_{30}\left[\left(\int_\Omega u^q\right)^{\frac{p}{q}+1}\right]^{\frac{l}{p+q}}\left(\int_\Omega u^{p+l}\right)^{\frac{p}{p+l}} \quad \text{on } (0, T_{max}).$$

The restriction $q > l$ implies $\frac{l}{p+q} + \frac{p}{p+l} < 1$, so that by invoking inequality (14) we can get for $\epsilon_7 > 0$

$$\int_\Omega u^l \int_\Omega u^p \le \epsilon_7 \int_\Omega u^{p+l} + \epsilon_7\left(\int_\Omega u^q\right)^{\frac{p+q}{q}} + c_{31} \quad \text{on } (0, T_{max}).$$

At this point, we can manipulate the term $\left(\int_\Omega u^q \right)^{\frac{p+q}{q}}$ as in (21). Rephrasing estimate (24) in terms of what derived, the same motivations used in Lemma 5.1 give the claim. □

Analysis of solutions to model (1) with $\tau = 1$; proof of Theorem 2.2.

Lemma 5.3. *For any $p > 1$ and $r, s > 2$, we have that u is such that for $\epsilon_8, \epsilon_9 > 0$*

$$(25) \quad \frac{d}{dt} \int_\Omega u^p \le (\epsilon_8 + \epsilon_9 - p(p-1)) \int_\Omega u^{p-2} |\nabla u|^2 + \int_\Omega |\nabla v|^r + \int_\Omega |\nabla w|^s + c_{33} \int_\Omega u^{\frac{pr}{r-2}} + c_{35} \int_\Omega u^{\frac{ps}{s-2}} \quad \text{for all } t \in (0, T_{max}).$$

Proof. Testing procedures imply the following estimate

$$(26) \quad \frac{d}{dt} \int_\Omega u^p = -p(p-1) \int_\Omega u^{p-2} |\nabla u|^2 + p(p-1)\chi \int_\Omega u^{p-1} \nabla u \cdot \nabla v - p(p-1)\xi \int_\Omega u^{p-1} \nabla u \cdot \nabla w \quad \text{on } (0, T_{max}),$$

whereas a twice application of Young's inequality infers for $\epsilon_8 > 0$ and for all $t \in (0, T_{max})$

$$(27) \quad p(p-1)\chi \int_\Omega u^{p-1} \nabla u \cdot \nabla v \le \epsilon_8 \int_\Omega u^{p-2} |\nabla u|^2 + c_{32} \int_\Omega u^p |\nabla v|^2 \le \epsilon_8 \int_\Omega u^{p-2} |\nabla u|^2 + \int_\Omega |\nabla v|^r + c_{33} \int_\Omega u^{\frac{pr}{r-2}},$$

and for $\epsilon_9 > 0$ on $(0, T_{max})$

$$(28) \quad -p(p-1)\xi \int_\Omega u^{p-1} \nabla u \cdot \nabla w \le \epsilon_9 \int_\Omega u^{p-2} |\nabla u|^2 + c_{34} \int_\Omega u^p |\nabla w|^2 \le \epsilon_9 \int_\Omega u^{p-2} |\nabla u|^2 + \int_\Omega |\nabla w|^s + c_{35} \int_\Omega u^{\frac{ps}{s-2}}.$$

The claim is deduced by simply plugging relations (27) and (28) into bound (26). □

Lemma 5.4. *Let either $l, k \in \left(0, \frac{1}{n} \right] = I$, or $l, k \in \left(\frac{1}{n}, \frac{1}{n} + \frac{2}{n^2+4} \right) = J$, or $l \in I$ and $k \in J$ (or viceversa). Then for some $p > \frac{n}{2}$ and some $L_1 > 0$, we have that u complies with*

$$\int_\Omega u^p \le L_1 \quad \text{for all} \quad t \in (0, T_{max}).$$

Proof. Let us set $p_0 = \frac{n}{2}$, $\rho_0 = \frac{2}{n}$ and $\phi(p, \rho, \sigma) := \frac{p\sigma}{\sigma-2} - (p+\rho)$, which is defined for all $p > 1$, $\rho > 0$ and $\sigma > 2$. Since for all $\sigma > \frac{n^2+4}{2}$ it happens that $\phi(p_0, \rho_0, \sigma) = \frac{n^2 - 2\sigma + 4}{n(\sigma-2)} < 0$, by continuity there are $p > p_0$ and $\rho < \rho_0$ such that $\phi(p, \rho, \sigma) < 0$, i.e.

$$(29) \quad \frac{p\sigma}{\sigma - 2} < p + \rho.$$

Being our scope controlling the terms $\int_\Omega |\nabla v|^r$, $\int_\Omega u^{\frac{pr}{r-2}}$ and $\int_\Omega |\nabla w|^s$, $\int_\Omega u^{\frac{ps}{s-2}}$ appearing in (25), let us take into consideration the regularity of v and w, and in particular the functional spaces where ∇v and ∇w belong, and let us study three different cases.

- Case $k, l \in I$. From Lemma 3.1, it is known that $\nabla v \in L^\infty((0, T_{max}); L^r(\Omega))$ and $\nabla w \in L^\infty((0, T_{max}); L^s(\Omega))$ for all $r, s > 1$, so that we may pick $r = s = \sigma > \frac{n^2+4}{2} > 2$, and by applying (29) we have for all $t \in (0, T_{max})$

$$(30) \quad p(p-1)\chi \int_\Omega u^{p-1} \nabla u \cdot \nabla v \le \epsilon_8 \int_\Omega u^{p-2} |\nabla u|^2 + \int_\Omega |\nabla v|^r + c_{33} \int_\Omega u^{\frac{pr}{r-2}} \le \epsilon_8 \int_\Omega u^{p-2} |\nabla u|^2 + \int_\Omega u^{p+\rho} + c_{36},$$

and on $(0, T_{max})$

$$(31) \quad -p(p-1)\xi \int_\Omega u^{p-1} \nabla u \cdot \nabla w \le \epsilon_9 \int_\Omega u^{p-2} |\nabla u|^2 + \int_\Omega |\nabla w|^s + c_{35} \int_\Omega u^{\frac{ps}{s-2}} \le \epsilon_9 \int_\Omega u^{p-2} |\nabla u|^2 + \int_\Omega u^{p+\rho} + c_{37}.$$

- Case $k \in I$ and $l \in J$ (or, viceversa, $k \in J$ and $l \in I$). We discuss the first situation, for which accordingly to Lemma 3.1, we have $\nabla v \in L^\infty((0, T_{max}); L^r(\Omega))$, for all $r \ge 1$ and $\nabla w \in L^\infty((0, T_{max}); L^s(\Omega))$ for all $1 \le s < \frac{n}{nl-1}$. (The second case is totally analogous.) Clearly estimate (30) still holds, while for the validity of bound (31) we need to make sure we can choose also $s = \sigma > \frac{n^2+4}{2}$, so to rely on (29). To this scope, it suffices to check that $\frac{n}{nl-1} > \frac{n^2+4}{2}$ for all $l \in J$. Since $\Lambda(l) := \frac{n}{nl-1}$ is decreasing in J and $\Lambda\left(\frac{1}{n} + \frac{2}{n^2+4} \right) = \frac{n^2+4}{2}$, we conclude.
- Case $l, k \in J$. By following for k the same arguments used previously for l, we can ensure that (30) and (31) are satisfied.

As a consequence of this, by putting bounds (30) and (31) into estimate (26) and by manipulating the term $\int_\Omega u^{p+\rho}$, with $\rho < \frac{2}{n}$ as the integral in (23), we are in the position to deduce. □

(a) Evolution in time of max u.

(b) Evolution in time of max u.

(c) Comparison of max u.
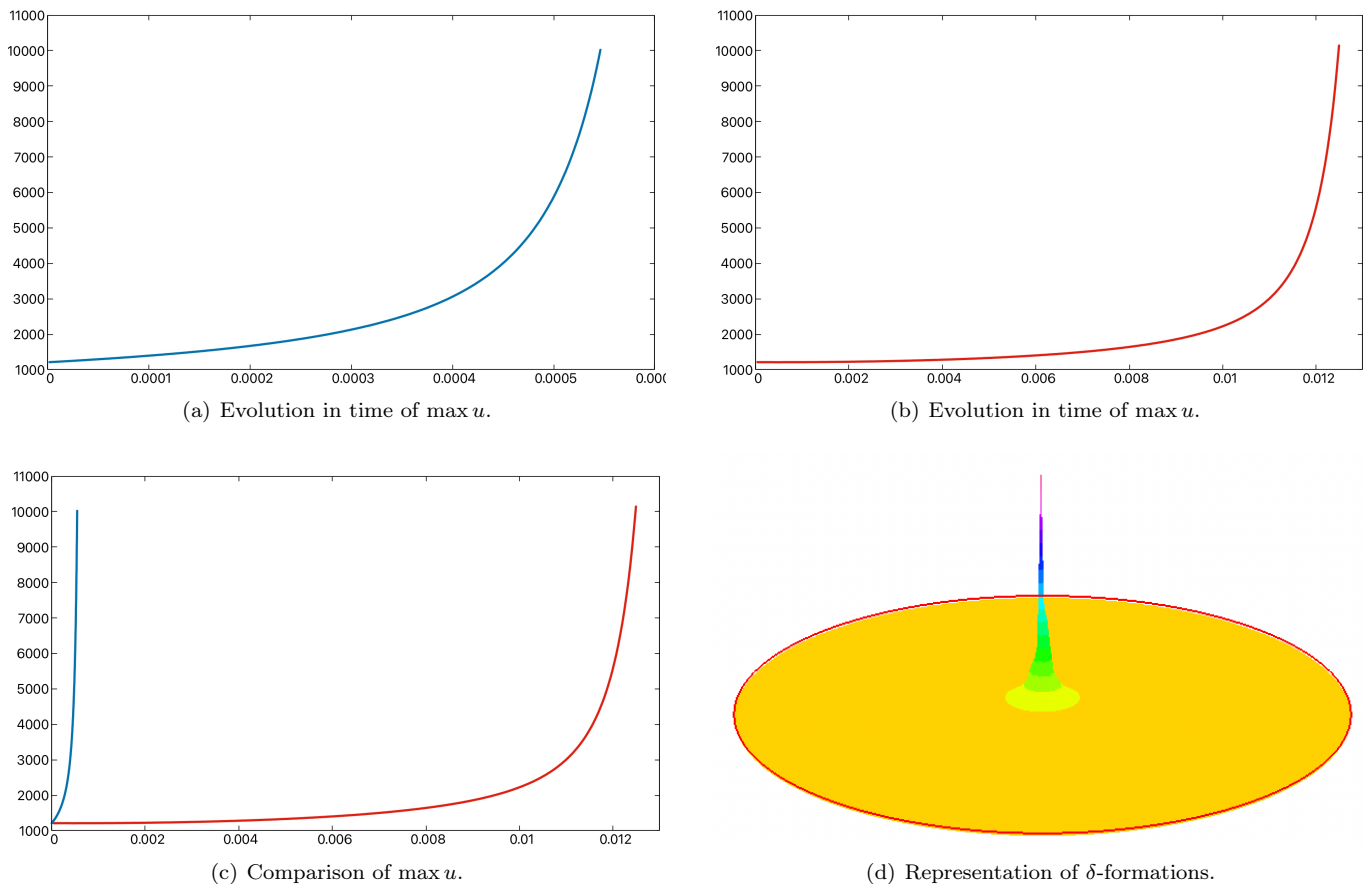
(d) Representation of δ-formations.

FIGURE 1. **Blow-up case.** Simulations of model (1) for $\tau = 0$ (blue color) and $\tau = 1$ (red color). Evolution of the cells' density: $T_{max} \approx 0.00054$ (top left), $T_{max} \approx 0.0012$ (top right), comparison of behaviors (bottom left), qualitative representation of finite time blow-up at a spatial point (bottom right). The quantitative values are indicated on the axes.

(a) Evolution in time of max u, max v and max w.
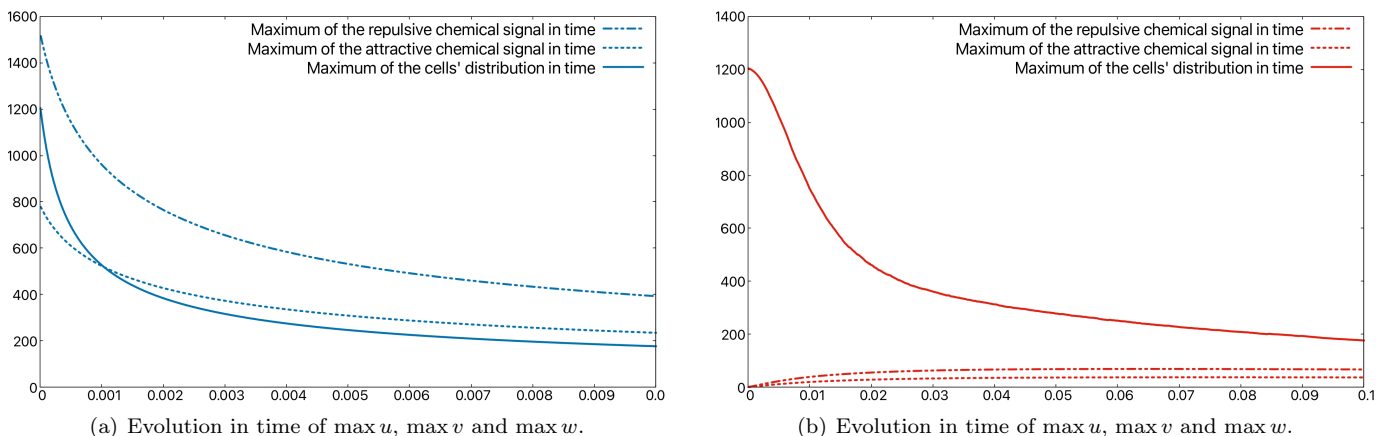
(b) Evolution in time of max u, max v and max w.

FIGURE 2. **Global boundedness case.** Simulations of model (1) for $\tau = 0$ (blue color) and $\tau = 1$ (red color). Evolution of the cells' density and the chemical signals. Whilst for $\tau = 1$, we have that max v_0 and max w_0 are given, for $\tau = 0$ they are computed accordingly to what said in Algorithm 1. The quantitative values are indicated on the axes.

6. NUMERICAL SIMULATIONS

Numerical simulations of taxis-driven models are by no means an easy goal and addressing technical and computational details connected with this analysis is a very challenging issue for the researchers in this field. This is essentially due to the fact that solutions to such systems may exhibit interesting mathematical properties (as for instance blow-up) which cannot

be easily reproduced in a discrete framework; indeed, spurious oscillations may appear during the simulations and this might lead to inconsistent results.

In this section we numerically test the presented theoretical results by simulating system (1) in two dimensions, for both the elliptic and parabolic version. The simulations are used to detect specific data and values of the parameters which delineate regions where different behaviors of solutions may manifest. We are, in particular, interested in two specific scenarios: solutions are bounded and their asymptotic behavior converges to a constant stationary solution, or they suffer from chemotactic blow-up in finite time.

To this aim we introduce a Finite Element Method (FEM) space discretization, defined on a triangular mesh of the domain Ω, with first order piecewise polynomials. On the other hand, we consider an implicit Euler scheme with time discretization Δt, and the algorithm at each time step consists of two operations: First we compute v and w as solutions of the (uncoupled) nonlinear equations in (1) modeling the segregation of these signals, being u explicitly given from the previous time step. Successively, the values of u at any node of the mesh are updated by solving the chemotaxis equation, exactly using the gained quantities of the repulsive and attractive substances at those nodes. Explicitly we have this

Algorithm 1. *Let j indicate the time step. For $j = 0, 1, \ldots$, we distinguish the cases $\tau = 0$ and $\tau = 1$:*
 ▷ *$\tau = 0$. Given u_j, we compute v_j and w_j. Then we obtain u_{j+1}, by using (u_j, v_j, w_j).*
 ▷ *$\tau = 1$. Given (u_j, v_j, w_j), we compute v_{j+1} and w_{j+1}. Then we obtain u_{j+1}, by using (u_j, v_{j+1}, w_{j+1}).*
As to the blow-up scenario, we fix this threshold criterion:
 ▷ *If for some j it holds that $\max u_j \geq 10^4$, then $T_{max} \approx j\Delta t$.*

The computations are developed by means of the the open source library FreeFem++ (see [5]).

6.1. **Comparing blow-up and boundedness scenarios for the cases $\tau = 0$ and $\tau = 1$.** We consider a mesh of the unit circle $\Omega = \{(x_1, x_2) \in \mathbb{R}^2 \mid x_1^2 + x_2^2 < 81\}$ composed by 43148 triangular elements, and a time discretization $\Delta t = 10^{-5}$. We take $\chi = \xi = 1$, $f(u) = \alpha u^k$, $\gamma_0 = \gamma_1$ and, thence, $g(u) = \gamma_0(1 + u)^l$, $\Theta_0 = \chi\alpha - \xi\gamma_0 = 0$ and the Gaussian bell-shaped initial values

$$\begin{cases} u_0(x_1, x_2) = 15e^{-(x_1^2 + x_2^2)}(81 - (x_1^2 + x_2^2)) & \text{if } \tau = 0, \\ u_0(x_1, x_2) = 15e^{-(x_1^2 + x_2^2)}(81 - (x_1^2 + x_2^2)), v_0(x_1, x_2) = w_0(x_1, x_2) = e^{-(x_1^2 + x_2^2)} & \text{if } \tau = 1. \end{cases}$$

Starting by highly spiky initial cells' density (whose value is 1215), our objective is finding production rates for the chemorepellent and chemoattractant so that either the value of such a spike becomes higher and the appearance of δ-formations is observed, or decreases and stabilizes. As to the first goal (for which we adopted an adaptive mesh refinement), we choose k, l outside the boundedness ranges in Theorems 2.1 and 2.2, and precisely $k = 1.1$ and $l = 0.9$. For both models ($\tau = 0$ and $\tau = 1$) it is seen (Figure 1) that the cell distribution uncontrollably increases, up to an explosion at finite time. Nevertheless, a significant difference between the corresponding values of the blow-up time is seen, and this difference can be well appreciated in Subfigure 1(c).

Oppositely, without changing u_0, we can prevent the previous singularity by suitably changing the values of k and l. Specifically, for $k = 1.1$ and $l = 1.2$ both models ($\tau = 0$ and $\tau = 1$) do not present any gathering effect and the cells and chemical densities remain bounded in time. We point out that the result obtained with these values of k and l is consistent with assumption (1) in Theorem 2.1, but it cannot be discussed in the frame of Theorem 2.2. Finally, Figure 2 quantifies the maximum values of u, v and w; in particular, it is possible to observe how the trend of the curves representing $\max u$, $\max v$ and $\max w$ approach the plateau and they become constant throughout the time. Actually (data not shown) they eventually achieve the constant equilibrium $(u, v, w) = \left(\frac{m}{|\Omega|}, \frac{\alpha}{\beta} \left(\frac{m}{|\Omega|} \right)^k, \frac{\gamma}{\delta} \left(1 + \frac{m}{|\Omega|} \right)^l \right)$, which manifestly solves the stationary problem

$$\begin{cases} 0 = \Delta u - \chi\nabla \cdot (u\nabla v) + \xi\nabla \cdot (u\nabla w) = \Delta v - \beta v + \alpha u^k = \Delta w - \delta w + \gamma_0(1 + u)^l & \text{in } \Omega \times (0, \infty), \\ u_\nu = v_\nu = w_\nu = 0 & \text{on } \partial\Omega \times (0, \infty). \end{cases}$$

6.2. **Analyzing the influence of the parameters k and l on T_{max}.** With Ω, Δt, $f(u)$, $g(u)$ and Θ_0 introduced above, in Table 1 we schematize heuristic analyses of some simulations by particularly indicating the value of the blow-up time for different initial configurations and some parameter sweep for k, l, Θ_0. The first row of the table was inserted to show the consistency of the numerical simulations with the theoretical conclusion of Theorem 2.1, when item (3) is considered. The other situations are of natural interpretation. The second and third row give hints about the increasing of the blow-up time when k decreases; in particular, for $k > l$, but $k < 1 \left(= \frac{2}{2}\right)$, gathering effects are appreciable. (Recall that for model (4), blow-up in planar domains is ensured for $k > l$ and $k > 1$.) If, indeed, we observe the part of the table dealing with the parabolic case, from the one hand boundedness is achieved for $k = l = 0.5$, accordingly to the assumption (1) of Theorem 2.2, but from the other hand the same might occur for higher values (fifth and seventh row). A further conclusion can be extrapolated by the fourth and sixth row: indeed, one can observe that whenever the initial distribution of the chemoattractant v_0 presents a higher maximum, the related blow-up time decreases.

	u_0	v_0	w_0	k	l	Θ_0	T_{max}
	$15e^{-(x_1^2+x_2^2)}(81-x_1^2-x_2^2)$			0.5	0.5	0.36	$+\infty$
$\tau=0$	$15e^{-(x_1^2+x_2^2)}(81-x_1^2-x_2^2)$			1.2	1	-0.2	0.00035
	$15e^{-(x_1^2+x_2^2)}(81-x_1^2-x_2^2)$			0.8	0.6	-0.64	0.0188
	$15e^{-(x_1^2+x_2^2)}(81-x_1^2-x_2^2)$	$e^{-(x_1^2+x_2^2)}$	$e^{-(x_1^2+x_2^2)}$	1	0.8	-0.2	0.025
$\tau=1$	$15e^{-(x_1^2+x_2^2)}(81-x_1^2-x_2^2)$	$e^{-(x_1^2+x_2^2)}$	$e^{-(x_1^2+x_2^2)}$	0.5	0.5	0.52	$+\infty$
	$15e^{-(x_1^2+x_2^2)}(81-x_1^2-x_2^2)$	$5e^{-(x_1^2+x_2^2)}$	$e^{-(x_1^2+x_2^2)}$	1	0.8	-0.2	0.022
	$15e^{-(x_1^2+x_2^2)}(81-x_1^2-x_2^2)$	$5e^{-(x_1^2+x_2^2)}$	$e^{-(x^2+x_2^2)}$	0.8	0.8	-0.58	$+\infty$

TABLE 1. Approximated values of T_{max} in terms of the sizes of k, l, Θ_0 and the initial data. With $T_{max} = +\infty$ we mean that the solution is globally bounded.

References

[1] H. Brezis. *Functional Analysis, Sobolev Spaces and Partial Differential Equations*. Springer-Verlag, New York, 2011.

[2] Y. Chiyo, M. Marras, Y. Tanaka, and T. Yokota. Blow-up phenomena in a parabolic-elliptic-elliptic attraction-repulsion chemotaxis system with superlinear logistic degradation. *Nonlinear Anal.*, 212:Paper No. 112550, 14, 2021.

[3] S. Frassu and G. Viglialoro. Boundedness for a fully parabolic Keller–Segel model with sublinear segregation and superlinear aggregation. *Acta Appl. Math.*, 171:Paper No. 19, 20, 2021.

[4] Q. Guo, Z. Jiang, and S. Zheng. Critical mass for an attraction-repulsion chemotaxis system. *Appl. Anal.*, 97(13):2349–2354, 2018.

[5] F. Hecht. New development in FreeFem++. *J. Numer. Math.*, 20(3-4):251–265, 2012.

[6] M. A. Herrero and J. J. L. Velázquez. A blow-up mechanism for a chemotaxis model. *Ann. Scuola Norm. Sup. Pisa Cl. Sci. (4)*, 24(4):633–683, 1997.

[7] L. Hong, M. Tian, and S. Zheng. An attraction-repulsion chemotaxis system with nonlinear productions. *J. Math. Anal. Appl.*, 484(1):123703, 8, 2020.

[8] D. Horstmann and M. Winkler. Boundedness vs. blow-up in a chemotaxis system. *J. Differerential Equations*, 215(1):52–107, 2005.

[9] W. Jäger and S. Luckhaus. On explosions of solutions to a system of partial differential equations modelling chemotaxis. *Trans. Amer. Math. Soc.*, 329(2):819–824, 1992.

[10] G. J. O. Jameson. Some inequalities for $(a+b)^p$ and $(a+b)^p + (a-b)^p$. *Math. Gaz.*, 98(541):96–103, 2014.

[11] E. F. Keller and L. A. Segel. Initiation of slime mold aggregation viewed as an instability. *J. Theoret. Biol.*, 26(3):399–415, 1970.

[12] E. F. Keller and L. A. Segel. Model for chemotaxis. *J. Theoret. Biol.*, 30(2):225–234, 1971.

[13] E. F. Keller and L. A. Segel. Traveling bands of chemotactic bacteria: A theoretical analysis. *J. Theoret. Biol.*, 30(2):235, 1971.

[14] O. A. Ladyženskaja, V. A. Solonnikov, and N. N. Ural'ceva. Linear and Quasi-Linear Equations of Parabolic Type. In *Translations of Mathematical Monographs*, volume 23. American Mathematical Society, 1988.

[15] J. Lankeit. Finite-time blow-up in the three-dimensional fully parabolic attraction-dominated attraction-repulsion chemotaxis system. *J. Math. Anal. Appl.*, 504(2):Paper No. 125409, 16, 2021.

[16] Y. Li and Y. Li. Blow-up of nonradial solutions to attraction-repulsion chemotaxis system in two dimensions. *Nonlinear Anal. Real World Appl.*, 30:170–183, 2016.

[17] D.-m. Liu and Y.-s. Tao. Boundedness in a chemotaxis system with nonlinear signal production. *Appl. Math. J. Chinese Univ. Ser. B*, 31(4):379–388, 2016.

[18] M. Liu and Y. Li. Finite-time blowup in attraction-repulsion systems with nonlinear signal production. *Nonlinear Anal. Real World Appl.*, 61:Paper No. 103305, 21, 2021.

[19] M. Luca, A. Chavez-Ross, L. Edelstein-Keshet, and A. Mogilner. Chemotactic signaling, microglia, and Alzheimer's disease senile plaques: Is there a connection? *Bull. Math. Biol.*, 65(4):693–730, 2003.

[20] M. Marras and G. Viglialoro. Boundedness in a fully parabolic chemotaxis-consumption system with nonlinear diffusion and sensitivity, and logistic source. *Math. Nachr.*, 291(14–15):2318–2333, 2018.

[21] M. S. Mock. An initial value problem from semiconductor device theory. *SIAM J. Math. Anal.*, 5:597–612, 1974.

[22] M. S. Mock. Asymptotic behavior of solutions of transport equations for semiconductor devices. *J. Math. Anal. Appl.*, 49:215–225, 1975.

[23] T. Nagai. Blowup of nonradial solutions to parabolic-elliptic systems modeling chemotaxis in two-dimensional domains. *J. Inequal. Appl.*, 6(1):37–55, 2001.

[24] L. Nirenberg. On elliptic partial differential equations. *Ann. Scuola Norm. Sup. Pisa Cl. Sci. (3)*, 2(13):115–162, 1959.

[25] K. Osaki and A. Yagi. Finite dimensional attractor for one-dimensional Keller–Segel equations. *Funkcial. Ekvacioj.*, 44(3):441–470, 2001.

[26] G. Ren and B. Liu. Global boundedness and asymptotic behavior in a quasilinear attraction–repulsion chemotaxis model with nonlinear signal production and logistic-type source. *Math. Models Methods Appl. Sci.*, 30(13):2619–2689, 2020.

[27] G. Ren and B. Liu. Boundedness and stabilization in the 3D minimal attraction-repulsion chemotaxis model with logistic source. *Z. Angew. Math. Phys.*, 73(2):Paper No. 58, 25, 2022.

[28] Y. Tao and Z.-A. Wang. Competing effects of attraction vs. repulsion in chemotaxis. *Math. Models Methods Appl. Sci.*, 23(1):1–36, 2013.

[29] Y. Tao and M. Winkler. Boundedness in a quasilinear parabolic-parabolic Keller–Segel system with subcritical sensitivity. *J. Differerential Equations*, 252(1):692–715, 2012.

[30] G. Viglialoro. Explicit lower bound of blow-up time for an attraction-repulsion chemotaxis system. *J. Math. Anal. App.*, 479(1):1069–1077, 2019.

[31] G. Viglialoro. Influence of nonlinear production on the global solvability of an attraction-repulsion chemotaxis system. *Math. Nachr.*, 294(12):2441–2454, 2021.

[32] M. Winkler. Aggregation vs. global diffusive behavior in the higher-dimensional Keller–Segel model. *J. Differerential Equations*, 248(12):2889–2905, 2010.

[33] M. Winkler. How far can chemotactic cross-diffusion enforce exceeding carrying capacities? *J. Nonlinear. Sci.*, 24(5):809–855, 2014.

[34] M. Winkler. A critical blow-up exponent in a chemotaxis system with nonlinear signal production. *Nonlinearity*, 31(5):2031–2056, 2018.

[35] H. Yu, Q. Guo, and S. Zheng. Finite time blow-up of nonradial solutions in an attraction-repulsion chemotaxis system. *Nonlinear Anal. Real World Appl.*, 34:335–342, 2017.

[36] X. Zhou, Z. Li, and J. Zhao. Asymptotic behavior in an attraction-repulsion chemotaxis system with nonlinear productions. *J. Math. Anal. Appl.*, 507(1):Paper No. 125763, 24, 2022.